
DECOMPOSING WEATHER FORECASTING INTO ADVECTION AND CONVECTION WITH NEURAL NETWORKS

A PREPRINT

Mengxuan Chen
Tsinghua University
chenmx21@mails.tsinghua.edu.cn

Ziqi Yuan
Tsinghua University
yzq21@mails.tsinghua.edu.cn

Jinxiao Zhang
Tsinghua University
zhang-jx22@mails.tsinghua.edu.cn

Runmin Dong
Tsinghua University
drm@mail.tsinghua.edu.cn

Haohuan Fu*
Tsinghua University
haohuan@tsinghua.edu.cn

ABSTRACT

Operational weather forecasting models have advanced for decades on both the explicit numerical solvers and the empirical physical parameterization schemes. However, the involved high computational costs and uncertainties in these existing schemes are requiring potential improvements through alternative machine learning methods. Previous works use a unified model to learn the dynamics and physics of the atmospheric model. Contrarily, we propose a simple yet effective machine learning model that learns the horizontal movement in the dynamical core and vertical movement in the physical parameterization separately. By replacing the advection with a graph attention network and the convection with a multi-layer perceptron, our model provides a new and efficient perspective to simulate the transition of variables in atmospheric models. We also assess the model's performance over a 5-day iterative forecasting. Under the same input variables and training methods, our model outperforms existing data-driven methods with a significantly-reduced number of parameters with a resolution of 5.625° . Overall, this work aims to contribute to the ongoing efforts that leverage machine learning techniques for improving both the accuracy and efficiency of global weather forecasting.

1 Introduction

Forecasting weather accurately is vital for human society. Numerical Weather Prediction (NWP), a dominant approach for weather forecasting, has been developed for more than 100 years Bauer et al. (2015). Benefited enormously from the advances in supercomputing capacity and observations, this revolution spans from parameterization schemes representing unresolved physical processes to data assimilation providing more precise initial states, from ensemble modeling addressing minor perturbations in initial conditions to increasing resolutions for eliminating uncertainties. Operational systems such as the Integrated Forecasting System (IFS) from the European Centre for Medium-Range Weather Forecasts (ECMWF) and the Global Forecast System (GFS) from the National Centers for Environmental Prediction (NCEP), play a crucial role in decision-making and risk management in everyday life.

A typical atmospheric model, such as the Community Atmosphere Model (CAM) or the Weather Research & Forecasting Model (WRF), typically comprises two parts: dynamical core and physical parameterization schemes. The Navier-Stokes equations, the mass continuity equations, and the governing equations of thermodynamics and ideal gas, form the foundation of numerical models in the dynamical core. In addition to these explicit equations, sub-grid or complex physical processes that cannot be resolved by the numerical models are calculated in the empirical-based physical parameterization schemes, such as the radiation transport and convection formation, as depicted in Figure 1. The combination of dynamics and physics forms the comprehensive atmospheric model. In pursuing a higher resolution and more precise description of the atmospheric state evolution, NWP faces challenges in terms of computational resources

*Correspondence to: H. Fu, haohuan@tsinghua.edu.cn

and the complex nonlinear system Randall (2013); Kriegmair et al. (2022). Consequently, these challenges promote the development of machine learning (ML), as a substitution method for traditional weather forecasting models.

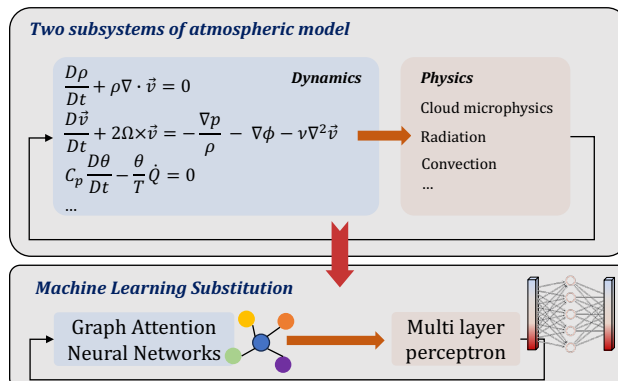


Figure 1: The combination of dynamics and physics forms the comprehensive atmosphere model. This study proposes a modularized weather forecasting model combining Graph Attention Network and Multi-Layer Perceptron (GAT-MLP) to simulate the advection and convection in the atmospheric model respectively, in an iterative forecasting manner.

In these years, we witnessed the great success of using ML in topics related to weather forecasting, including but not limited to the data assimilation, substitution of climate models, and the correction of the model output Buizza et al. (2022); Bonavita and Laloyaux (2020); Watt-Meyer et al. (2021). Starting from using Multi-Layer Perceptron (MLP) to simulate the complex nonlinear physical processes within each vertical column (grid with different pressure levels), ML shows great potential in learning intricate relationships from huge amount of data. To address the limitation that MLP cannot explicitly learn the spatial relationship between grids, Convolutional Neural Networks (CNN) are then introduced and widely used in weather forecasting to achieve better performance and higher computational efficiency. However, the characteristic of CNN viewing the atmospheric status as an image with multiple channels, is not in line with the real case. For instance, transferring information from the leftmost side to the rightmost side in an image poses challenges, and is only performed in the deep layers in CNN-based models, despite the expectation of continuity in the real world. Furthermore, there is no specific guarantee of the boundaries in the image, such as the north and south poles. Also, the convolutional kernels assume the translation invariance in the image, which is not always correct in reality. For example, the increase in sea surface temperature (SST) may have different impacts on its east and west coast Palmer and Mansfield (1984). To address the issues mentioned above, attention mechanisms, Transformer or Graph Neural Networks (GNN) are introduced in the weather forecasting task, to learn a better relationship between variables exchange at different locations. Particularly, GNN can explicitly model the interactions and variable transfer between the nodes by designing specific graph structures, which is more interpretable Liu et al. (2022), and has gained attention in recent years Keisler (2022); Lam et al. (2023).

Among all the successful studies using ML methods for weather forecasting, most try to use one unified neural network to represent both dynamics and physical processes in the atmospheric model. These models are meticulously designed to extract useful information from vast amounts of training data. Consequently, they experience exponentially-increased parameters when pursuing more accurate results. Simultaneously, the lack of interpretability of these complex models make it difficult to express the working mechanisms. Since atmospheric models have a long development history, it is another choice to draw inspiration and learn from the accumulated experience and insights instead of completely discarding the original methods when utilizing ML for substitution.

Therefore, in this work, as shown in Figure 1, we propose a simple yet effective model to learn and represent the dynamics and physics of the atmospheric model as two separate neural networks. Figure 2 shows a general workflow of our proposed model. Compared with previous works, our model provides the following unique features:

- **A divide-and-conquer modeling approach.** Different from using a comprehensive model to unify all the processes in the atmospheric model, our model uses two components to learn the advection in dynamical core and convection in physical parameterization part separately. We adopt a Graph Attention Network (GAT) Veličković et al. (2018) to emulate the advection between the nodes and their connected neighbors and an MLP to simulate the physical processes within each vertical column.
- **Stencil-like graph structure.** Different from first mapping the grid data onto the icosahedron mesh, we directly model each latitude-longitude (lat-lon) grid as an independent node, and connect each node with its

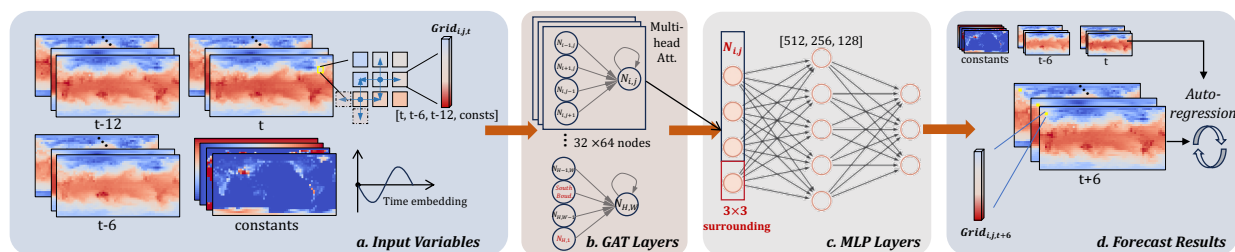


Figure 2: A general view of our proposed model. Variables from the previous three timesteps and the constants are input variables. Each grid is viewed as a node and connected with four neighbors. Then, the whole graph is put into a 2-layer Graph Attention Network (GAT), followed by a 4-layer Multi-Layer Perceptron (MLP) to predict the variables in the next timestep. This model adopts the auto-regressive manner for prediction, which means, the predicted variables are fed back into the model for iterative forecasting.

four neighbors through graph edges. Besides, two boundary nodes are set to define the north and south poles to ensure the closure of the graph structure.

- **Non-local physical process simulation.** Different from MLP models that perform in every vertical column, we integrate information from surrounding 3×3 grids to simulate the physical process with non-local MLP.

Moreover, in contrast to existing models, our model is lightweight with only 4.38M parameters in total for a resolution of 5.625° .

2 Literature Review

2.1 Machine Learning in Weather Forecasting

Operational weather forecasting typically involves data preparation, data assimilation, prediction, postprocessing, and results evaluation. In order to replace the time-consuming computational process and better capture the non-linear relationship in atmospheric variables, ML-based weather forecasting models in current stage aim to replace the entire process except for data preparation and results evaluation Schultz et al. (2021).

The availability of extensive datasets like ERA5 Hersbach et al. (2018) and model data from CMIP projections Eyring et al. (2016) have significantly contributed to the growth of machine learning applications in weather forecasting and climate modeling, particularly in end-to-end workflows. At the very beginning, MLP and CNN are the most commonly used methods Rasp et al. (2020); Weyn et al. (2020); Rasp and Thuerey (2021); Clare et al. (2021). In recent years, more advanced methods have been gradually adopted in weather forecasting with the development of both computer vision techniques and hardware. In order to capture the temporal dependence, methods such as Recurrent Neural Networks (RNN) and Long Short-Term Memory (LSTM) are added to the network Espeholt et al. (2022); Chen et al. (2023a). To model the long-range dependencies well, newly-developed models tend to use Transformer as the backbone to extract features Pathak et al. (2022); Bi et al. (2023); Nguyen et al. (2023); Chen et al. (2023b). Besides, some studies have demonstrated the potential of utilizing Graph Neural Networks for large-scale and long-term weather forecasting Keisler (2022); Lam et al. (2023) and using diffusion models for the ensemble prediction Price et al. (2023).

2.2 Graph Neural Networks in Earth Systems

Graph Neural Networks (GNN) was initially proposed to deal with unstructured data, which needs to be represented in graph domains Scarselli et al. (2008). By learning node representations through iterative message-passing between interconnected nodes several times, GNN can capture complex dependencies and intricate interconnections within a graph. GNNs have gained growing attention over the past five years for their effectiveness in modeling the Earth system’s dynamic mechanisms and variable exchanges. Starting with its application to enhance El Niño forecasting Cachay et al. (2020), GNNs have demonstrated their potential and aptness in modeling *grid* climate data. This becomes particularly pertinent in scenarios where the current state in one grid is significantly influenced by the states from the neighbors.

After that, GNN and graph convolutional networks (GCN) are tested to simulate atmospheric radiative transfer in weather and climate models. The findings indicate that graph-based networks exhibit a smaller mean biased error and

greater flexibility when compared to models constructed with CNN and MLP Cachay et al. (2021). In 2022, Keisler employs the GNN for global weather forecasting Keisler (2022). The study demonstrates that message-passing GNN outperformed CNN-based weather forecasting models in terms of both accuracy and model size during a 6-day iterative running. Additionally, the GNN performance was comparable to that of the European Centre for Medium-Range Weather Forecasts (ECMWF) model. As a superior follow-up, the GraphCast model elevates the GNN-based medium-range global weather forecasting to a new level, and outperforms ECMWF’s High RESolution forecast (HERS), one of the most accurate operational deterministic systems in the world Lam et al. (2023). Both of the above-mentioned works project the climate data onto the icosahedron meshes to eliminate the artifacts of discontinuity and no specific north and south poles in the original lat-lon grid data.

Beyond these works, GNNs have been applied in many other fields, such as the heatwave prediction Li et al. (2023), river network learning Sun et al. (2022), hourly solar radiation prediction Gao et al. (2022), and $PM_{2.5}$ forecasting Wang et al. (2020). The works mentioned above show that GNN has great potential in applications related to the Earth systems, especially in learning the relationships between different variables and locations.

3 Approach

3.1 Model Architecture

The complete workflow for our weather forecasting model includes a grid-to-node encoder, a GAT-MLP model to simulate the advection and convection in the atmospheric models, and a node-to-grid forecast module, as depicted in Figure 2.

Grid-to-Node Encoder The grid-to-node encoder is designed to formulate each grid with different pressure levels in the lat-lon coordinate as a node in the graph, and the neighborhood relationship between them is represented with graph edges, as shown in Figure 2(a). We use data from previous three time steps as the major input variables. Different from previous GNN-based weather forecasting approaches Keisler (2022); Lam et al. (2023) that first project the original lat-lon grid ERA5 data onto icosahedron meshes with various resolutions, our model directly employs the lat-lon grid to eliminate the errors introduced by mesh transformation. The input variables are encoded as the node features.

We formulate the node’s edges according to the 2D stencil computation. For a given node $N_{i,j}$ located in line i and column j , it connects to its four neighbours $N_{i-1,j}$, $N_{i+1,j}$, $N_{i,j-1}$, $N_{i,j+1}$ to simulate the five-point stencil calculation. Besides, we connect nodes $N_{:,0}$ to $N_{:,\mathbb{W}-1}$ to ensure continuity, align with the real world. The nodes $N_{0,:}$ and $N_{\mathbb{H}-1,:}$ are linked to pseudo nodes representing the north and south poles, respectively, to ensure the closure. H and W denote the total number of grids in the latitude and longitude directions, which, in this case, are 32 and 64 for 5.625° resolution. The variables are encoded as node features, with the pseudo nodes having all-zero values. The node features are then fed into the GAT. Appendix B provides a detailed explanation of this process.

GAT-MLP Model Structure In the atmospheric model, the dynamical core uses numerical methods to transform the atmospheric governing equations into discrete forms, and stencil calculation is used for calculating the fluxes in and out from neighboring grids. Some atmospheric variables that cannot be solved at the grid scale or be described by the atmospheric equations are represented by the physical parameterization schemes, which are calculated within each vertical column and do not exchange with neighboring grids. Inspired by the success of GNN in weather forecasting and of MLP in subgrid physical process representation, as well as the running mechanisms in atmospheric models, our model is primarily composed of two parts: a 2-layer GAT to simulate the advection between interconnected nodes, and a 4-layer MLP to mimic the convection within each vertical column, as illustrated in Figure 2 (b-c).

GAT Layer: For a given node N_i and one of its neighbour N_j , the attention coefficient first computes the similarity factor between itself and its neighbour with

$$\alpha_{i,j} = \frac{\exp(\text{LeakyReLU}(f(W \cdot N_i || W \cdot N_j)))}{\sum_{j \in J} \exp(\text{LeakyReLU}(f(W \cdot N_i || W \cdot N_j)))}, \quad (1)$$

where W is the shared weighted matrix, $||$ denotes the concatenate process, and J is the set of N_i ’s neighbours, with a self-loop embedding. Then, the neighbour information is aggregated to N_i to update its feature with

$$N'_i = \sigma\left(\sum_{j \in J} \alpha_{i,j} W' N_j\right), \quad (2)$$

where σ is the activation function. In this work, we use the multi-head attention mechanism to improve the model performance by setting the number of heads to 8. Therefore, for each head, it gives the updated feature N'_i with

$$N'_i(k) = \sigma\left(\sum_{j \in J} \alpha_{i,j}^k W'^k N_j\right), \quad (3)$$

for k is the head index. We use a two-layer GAT to simulate the exchange process between interconnected nodes. Currently, the vertical dependence in dynamical part is not explicitly modeled, and we assume that the MLP layer will capture part of the dependence.

MLP Layer: A four-layer MLP with hidden dimensions of 512, 256 and 128 is used for the second stage, as previous studies showed that MLP with shallow layers is enough to simulate the physical process within vertical columns Brenowitz and Bretherton (2018); Rasp et al. (2018); Yuval and O’Gorman (2023); Watt-Meyer et al. (2024) Besides, Wang et al. (2022) has demonstrated that adding surrounding 3×3 neighboring information help increase the performance. Therefore, for each node, the features from surrounding 3×3 nodes are extracted with the one-layer CNN with the kernel size of 3×3 , and encoded into 256 hidden dimensions. Then, the extracted features are concatenated with the node features, and fed into the MLP network to simulate the physical process within each vertical column. The output of the MLP layer is the predicted variables at the next time step.

Node-to-Grid Forecast The node-to-grid forecast module is shown in Figure 2(d), which converts the graph structure to the original lat-lon coordinate. The same as the operational weather forecasting model, our proposed model follows the auto-regression forecast scheme. We use iterative forecasting with a step of 6 hours in the experiment. For example,

$$z_{t+12} = \text{Model}(\text{Model}(z_t, z_{t-6}, z_{t-12}, \text{consts}), z_t, z_{t-6}, \text{consts}).$$

The forecast process is repeated until the desired lead time is reached. While iterative prediction may exhibit decreased performance compared to direct or continuous forecasts used in many studies attributed to the accumulation of prediction errors, it offers a more realistic approach to support long-term operations.

3.2 Data Preprocessing

Time and Location Embedding As for the constant variable latitude and longitude in WeatherBench dataset, we embed the latitude and longitude as

$$\text{lat} = \cos \frac{2\pi(h + 90)}{180}, \text{lon} = \sin \frac{2\pi w}{360},$$

where $h \in [-90^\circ, 90^\circ]$ and $w \in [0^\circ, 360^\circ]$. Besides, the time is encoded as

$$t' = -\sin \frac{2\pi}{T} t,$$

where T is the total hours in each year, and t is the specific hour in that year.

Data Normlization We apply instance normalization Ulyanov et al. (2017) to our input variables, using mean and standard deviation values calculated from the corresponding time steps for normalization. Variational mean and standard deviation values aim to enhance the model’s robustness, particularly in adapting to scenarios like climate change, where temperature increases may introduce greater variability.

3.3 Iterative Training

We train our model for 150 epochs, with an initial learning rate of 0.001 and the AdamW optimizer. The loss function used is the latitude-weighted RMSE, where the latitude-weight is represented as

$$L(h) = \frac{\cos(h)}{1/H \sum_{\text{lat}=1}^H \cos(\text{lat})} \quad (4)$$

The learning rate is reduced by a factor of two after every ten epochs. During the initial 100 epochs, the model is trained to forecast 6 hours ahead (forecasting one step). Subsequently, epochs 101-125 are dedicated to forecasting 30 hours ahead (forecasting five steps), epochs 126-140 are used for 54 hours ahead (forecasting nine steps), and the final ten epochs are focused on forecasting 78 hours ahead (forecasting 13 steps). The multistep training process aims to improve the iterative forecasting performance.

4 Experiments and Results

4.1 Data

We employ WeatherBench1, a widely used preprocessed dataset for weather forecasting based on ECMWF’s ERA5 dataset Rasp et al. (2020); Hersbach et al. (2018). We use the 5.625° resolution data from 1980 to 2018, with a sampling interval of 10 hours, and set the proportion of training, validation and test dataset to 8:1:1. Table 1 lists the variables used in our model.

Table 1: WeatherBench variables used in the model. Below the divider line are the constants.

Variable	Abbr.	Pressure levels
geopotential	z	Multi-levels ¹
temperature	t	Multi-levels
u_component_of_wind	u	Multi-levels
v_component_of_wind	v	Multi-levels
vorticity	vo	Multi-levels
specific_humidity	q	Multi-levels
2m_temperature	t2m	Single level
total_precipitation	tp	Single level
land-sea mask	lsm	/
Orography	h	/
latitude location	lat2d	/
longitude location	lon2d	/

¹ Multi-levels refer to 50, 250, 500, 600, 700, 850, 925 [hPa]

For our chosen subset of WeatherBench1, geopotential height can provide valuable information about the vertical structure, pressure distribution, and large-scale circulation of the atmosphere. u and v component of wind and vorticity are fundamental parameters in weather forecasting, providing critical information about the movement, convergence, and divergence of air masses, while 2m temperature is essential for human activity. Variables at time t , $t - 6$, and $t - 12$ are used as the input, and the task involved forecasting these variables at a lead time up to 120 hours iteratively, with an interval of 6 hours. Including variables from multiple time steps may help the model to capture the time dependencies and diurnal cycles, simultaneously having a more robust and stable performance in iterative forecasting tasks.

4.2 Evaluation Metrics

The evaluation metrics are latitude-weighted RMSE and Anomaly Correlation Coefficient (ACC), as described in Equation 5 and 6.

$$RMSE = \frac{1}{N} \sum_{t=1}^N \sqrt{\frac{1}{HW} \sum_{h=1}^H \sum_{w=1}^W L(h)(y_{t,h,w} - \hat{y}_{t,h,w})^2} \quad (5)$$

$$ACC = \frac{\sum_{t,h,w} L(h)y'_{t,h,w}\hat{y}'_{t,h,w}}{\sqrt{\sum_{t,h,w} L(h)(y'_{t,h,w})^2} \sqrt{\sum_{t,h,w} L(h)(\hat{y}'_{t,h,w})^2}} \quad (6)$$

where $L(h)$ is the latitude-weight shown in Equation 4. y' and \hat{y}' are respectively the anomalies of y and \hat{y} against the climatology $C_{h,w} = \frac{1}{N} \sum_{t=1}^N y_{t,h,w}$ at each grid.

4.3 Global Forecasting Results

We assess the model performance in global weather forecasting. We report the metrics scores of geopotential at 500 hPa (Z500), temperature at 850 hPa (T850), and temperature near surface (T2M), and show the results of iterative forecasting. Figure 3 provides a visual example of the global forecasting results. For each variable, the first row shows the prediction and the second row represents the ground truth from the WeatherBench dataset. While from the ERA5 data, Z500 does not exhibit significant variations in a short term, T850 and T2M show clear diurnal cycles as the

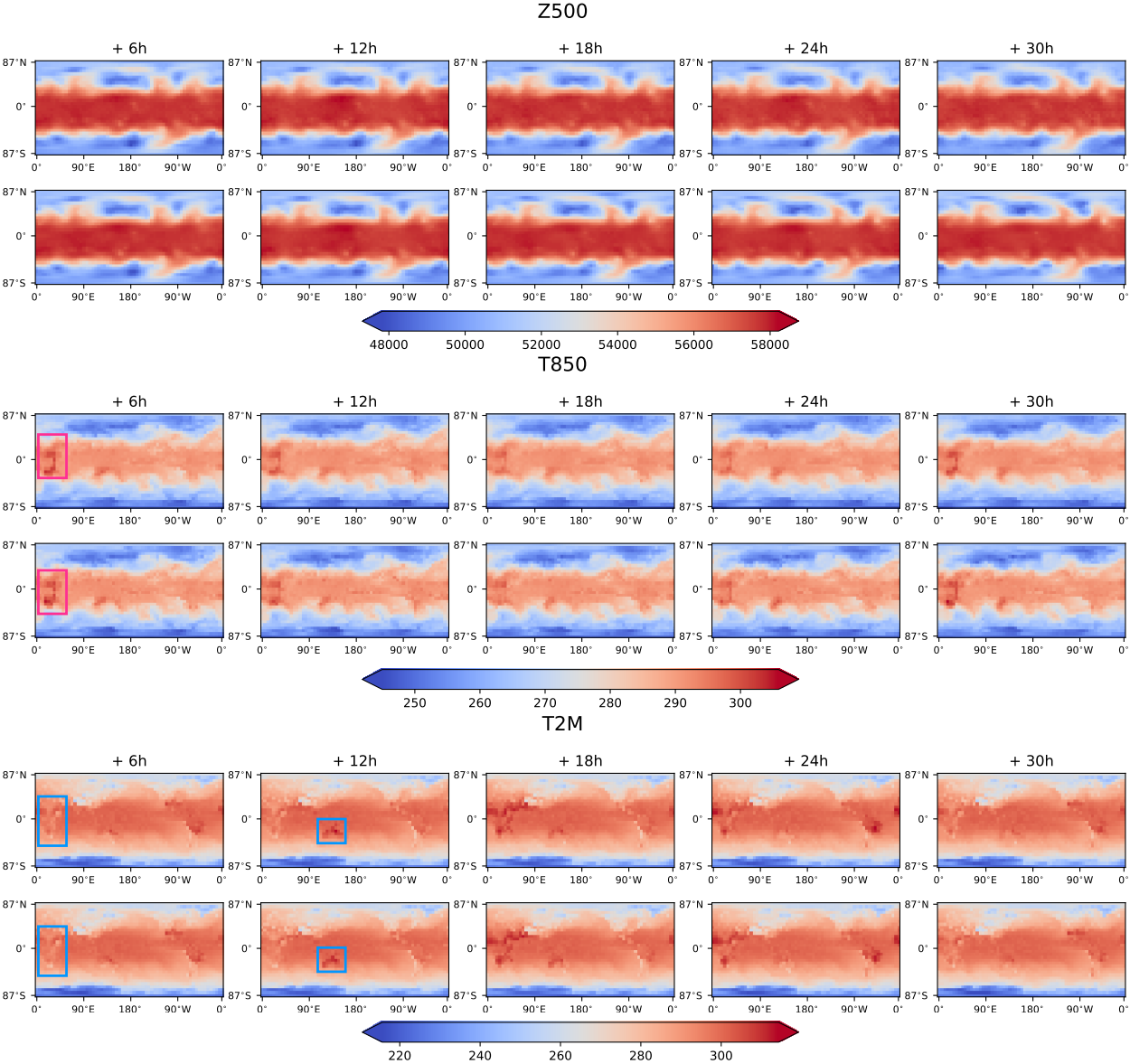


Figure 3: An example of the visualization of global forecasting results with 30 hours lead time of Z500, T850, and T2M. For each variable, the first row shows the predicted results by our model, and the second row shows the ground truth from WeatherBench dataset.

forecast progresses, particularly noteworthy in regions such as Africa and Australia, highlighted by the pink and blue boxes in the figure. Our model successfully captures the intricate global atmospheric patterns well, and their changing cycles over time.

4.4 Ablation Study

We assess the effectiveness of our model with the ablation study. The results for one-step prediction for Z500, T850, T2M and Total Precipitation (TP) are shown in Table 2, and the whole iterative forecasting performance with a 5-day lead time is shown in Figure 4.

Two baselines are set up to test the primary performance that can be obtained by using either GAT or MLP. The first baseline is a 2-layer GAT with 8 heads and 128 hidden units, denoted as *GAT*. The second one is a four-layer MLP with 512, 256, and 128 hidden units, denoted as *MLP*. From the results, the GAT forecasting results in T2M vibrate

Table 2: Ablation study results for one-step prediction.

				Z500		T850		T2M		TP	
				RMSE↓	ACC↑	RMSE↓	ACC↑	RMSE↓	ACC↑	RMSE↓	ACC↑
✓				135.91	0.99	1.34	0.97	2.76	0.89	0.38	0.54
	✓			178.26	0.99	1.44	0.96	2.07	0.94	0.39	0.52
✓	✓			116.01	0.99	1.24	0.97	1.53	0.97	0.37	0.56
✓	✓	✓		116.49	0.99	1.23	0.97	1.52	0.97	0.37	0.56
✓	✓	✓	✓	96.30	1.00	1.12	0.98	1.38	0.97	0.36	0.61
GAT	MLP	+ time&loc.	+ surr. info.								

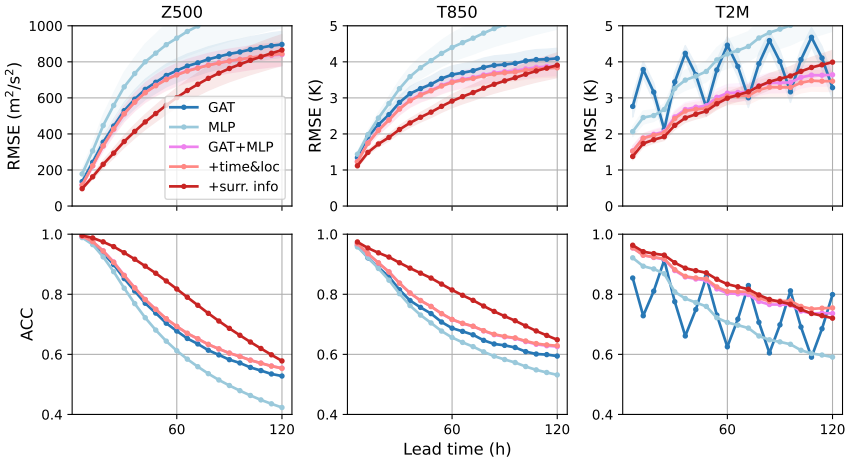


Figure 4: Ablation study results for 5-day iterative forecasting.

with the iterations, which means it can not capture the diurnal variations. In addition, the results for single MLP become divergent after several iterations. Using either component to simulate the weather forecasting process is still challenging.

By contrast, the combined model can alleviate the above-mentioned problems, and enhance the forecasting performance. *+time&loc.* involves the time and location embeddings described in Section 3.2. Adding the time and location embeddings does not have much impact on the performance of Z500 and T850 (as two lines describing *GAT+MLP* and *+time&loc.* in Figure 4 are overlapped). However, it can improve the forecasting of T2M after several iterations. This may indicate that the time embeddings can improve the learning of the temperature diurnal cycle. *+surr. info.* indicates the inclusion of surrounding information from neighboring 3×3 grids. Adding the information from neighbors can improve the model’s performance within the iterative prediction of 5 days. However, the performance decays as the iteration continuous. The possible reason is that the uncertainty in surrounding information hampers the model’s performance in long-term forecasting.

4.5 Validation of Iterative Training

To validate the improvement brought about by the iterative training process, we train the model for 150 epochs only to forecast 6 hours. The results shown in Figure 5 show the efficacy of the iterative training strategy. Although single-step training has comparable performance with iterative training on the first two time steps, and even surpasses the Z500 at a forecast time at 6 hours, it is less robust than iterative prediction in medium-range weather forecasting.

4.6 Comparison of different graph edges

We compare the performance of connecting the surrounding four nodes (five edges including a self-loop) and the surrounding eight nodes (nine edges) in our model, since, intuitively, connecting with all eight neighbors will incorporate more information in the dynamic processes, such as the wind blowing from northeast to southwest. The results are

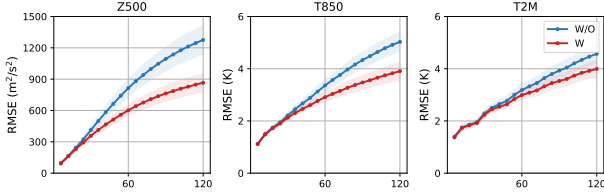


Figure 5: Validation of the iterative training strategy. W and W/O refer to with and without iterative training strategy.

shown in Figure 6. Five-edge connection performs better than nine-edge connection in Z500 and T850, but not so well in T2M after five forecasting steps.

There are two reasons for us to adopt the five-edge structure. The first is that it demonstrates better performance in an overall situation. The second is from both data and atmospheric model levels. Since the horizontal winds in the atmospheric model, as well as the ERA5 dataset we used, are the meridional wind and zonal wind, we would like to follow the design of the Arakawa C-grid Arakawa and Lamb (1977), a widely used grid in modern atmospheric or weather forecasting models. In this case, the natural wind direction in each grid is calculated with meridional and zonal winds by the trigonometric function. Besides, the wind is the basic prognostic variable in the atmospheric model, and other factors, such as water vapor and aerosol, are transmitted by the wind. Therefore, using four nodes can describe the data given, while eight nodes will increase the uncertainty of variables when projected to the meridional and zonal direction.

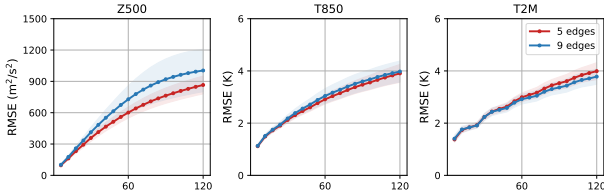


Figure 6: Comparison of graph with five edges and nine edges.

4.7 Analysis of different GAT layers

GNNs have suffered from the over-smoothing problem, which means the node representations are indistinguishable during the message-passing process when multi-layers are stacked Chen et al. (2020). Therefore, we test the performance of the proposed model with different graph attention layers ranging from 2 to 5, while other parts remain identical. The results are shown in Figure 7.

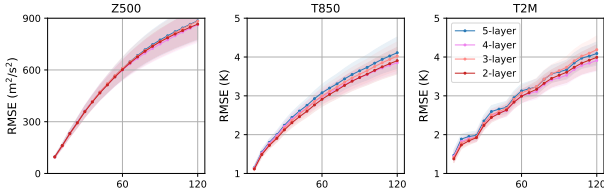


Figure 7: Analysis of the effects of different GAT layers.

The results demonstrate that while GAT with two layers performs best in the first 12 steps for Z500 and T2M, and the first 17 steps for T850, GAT with four layers is more stable in a long-term forecast. However, there is no significant difference in the performance of GAT across different layers.

4.8 Competing Methods

We conduct a comparative analysis of our model against several benchmark models, including a CNN-based model WeatherBench Rasp et al. (2020), a graph-based model Keisler (2022), and a Transformer-based model ClimaX Nguyen et al. (2023). These models vary in terms of the number of parameters and network scales. We train all these models from scratch using the same variables and training methods in this study to ensure the fairness and comparability of

the results. One-step forecasting results are summarized in Table 3, and Figure 8 compares the iterative forecasting performance. Our model outperforms these competing models according to these three variables, and is comparable to ClimaX with a much smaller number of parameters. We also include the NWP results from the Integrated Forecasting System ECMWF in Table 3. As expected, our method is not comparable to IFS at the current stage, and we will continuously refine our model in the future from both the model structure and the training method.

Table 3: Comparison with competing methods for one-step prediction.

	Z500		T850		T2M		TP		Parameters (M) ¹
	RMSE↓	ACC↑	RMSE↓	ACC↑	RMSE↓	ACC↑	RMSE↓	ACC↑	
Rasp et al. (2020)	413.98	0.93	2.62	0.88	3.66	0.82	0.42	0.39	6.37
Keisler (2022)	234.38	0.98	1.58	0.96	2.75	0.89	0.53	0.32	7.94
Nguyen et al. (2023)	129.47	0.99	1.39	0.97	2.21	0.94	0.36	0.6	108.98
Ours	96.30	1.00	1.12	0.98	1.38	0.97	0.36	0.61	4.38
IFS	26.93	1.00	0.69	0.99	0.97	0.99	/	/	/

¹ Parameters in blue may be different from the original paper due to the adjustment for hyperparameters.

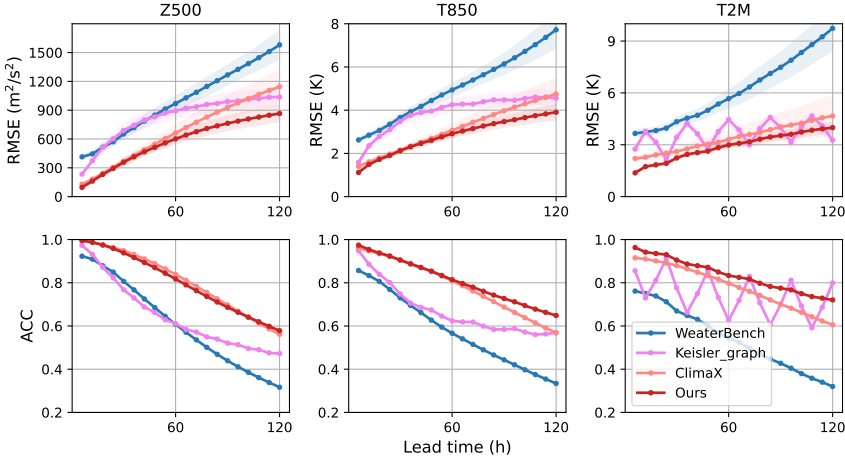


Figure 8: Comparison with competing methods for 5-day iterative forecasting.

The discrepancy between our reproduced results and those in the original works can mainly be attributed to the different training methods, dataset composition, and resolution. For example, ClimaX initially incorporates an extensive volume of data from CMIP6 for pretraining, while we only use the ERA5 data to train it from scratch. Besides, the difference in training datasets introduces variations in learned representations. Keisler (2022) uses single timestep variables (78 variables with 1° resolution) as the input, while we used variables from the previous three timesteps (137 variables with 5.625° resolution). The decreased resolution may result in sparse information when mapped to the icosahedron mesh with a total number of 5,882 cells, and the information becomes over-smoothing after nine rounds of message-passing GNN.

To sum up, according to the results of both the ablation study and the comparison with competing methods, our proposed GAT-MLP model can well capture the global atmospheric patterns, and reflect the variation of temperature diurnal cycle with a much smaller number of parameters. It also shows the great potential of using the combination of graph and MLP to simulate the dynamics and physics process in weather forecasting by learning the intricate interactions between the variables and locations.

5 Discussion

In this work, we proposed a simple yet effective two-stage GAT-MLP network to simulate the weather forecasting process. The first component is a 2-layer GAT to simulate the advection between the interconnected neighbors. The second component is a 4-layer MLP to learn the convection within each vertical column. Previous studies prefer to use a unified model to substitute the whole weather forecasting process, and most of them discarding the original development

of numerical models, while we split the network into two parts after rethinking the effectiveness of integrating the dynamics and physics in the atmospheric model. This work demonstrates the potential of using a lightweight model to represent the complex process in atmosphere by learning from numerical models. However, there are still some limitations that require further investigation.

Resolution The resolution of the data is 5.625° , which is not comparable to the results from the operational weather forecasting models such as ECMWF’s IFS and NOAA’s GFS in terms of both resolution and accuracy. Although 5.625° resolution is able to describe the general global weather patterns with minimal information loss Rasp et al. (2020), and can validate the effectiveness of our proposed method, it may fall short of capturing the small-scale weather phenomena. Several studies point out that the model performance will be enhanced with the increase in data resolution Rasp and Thuerey (2021); Nguyen et al. (2023). However, it is also challenging to push the resolution to a higher level due to the computational costs and memory limitations.

Physical Meanings Currently, all these variables are put into the model at the very beginning without considering the physical meanings, the explicit vertical dependence in stencil calculation, and the sequential order of variable calculation in a real atmospheric model. In the future, we would like to split the variables according to their association with the dynamic core and physical processes, such as the recently published work Kochkov et al. (2023). For example, variables like wind components predominantly rely on the dynamic core for calculation, while precipitation and radiation are calculated in the physical processes. Also, physical meanings can be added to the GAT layers to ensure the conservation. The future direction aligns with our commitment to refine the model’s representation of the atmospheric model and enhance its consistency with the physical constraints.

In summary, this work explores the potential of decomposing the weather forecasting model into advection and convection. Specifically, the flexibility of graph structures has provided our model with significant room for development, which we will explore in the future.

References

- Peter Bauer, Alan Thorpe, and Gilbert Brunet. The quiet revolution of numerical weather prediction. *Nature*, 525(7567):47–55, 2015.
- Caterina Buizza, César Quilodrán Casas, Philip Nadler, Julian Mack, Stefano Marrone, Zainab Titus, Clémence Le Cornec, Evelyn Heylen, Tolga Dur, Luis Baca Ruiz, et al. Data learning: Integrating data assimilation and machine learning. *Journal of Computational Science*, 58:101525, 2022.
- Massimo Bonavita and Patrick Laloyaux. Machine learning for model error inference and correction. *Journal of Advances in Modeling Earth Systems*, 12(12):e2020MS002232, 2020.
- Oliver Watt-Meyer, Noah D Brenowitz, Spencer K Clark, Brian Henn, Anna Kwa, Jeremy McGibbon, W Andre Perkins, and Christopher S Bretherton. Correcting weather and climate models by machine learning nudged historical simulations. *Geophysical Research Letters*, 48(15):e2021GL092555, 2021.
- Lasse Espeholt, Shreya Agrawal, Casper Sønderyby, Manoj Kumar, Jonathan Heek, Carla Bromberg, Cenk Gazen, Rob Carver, Marcin Andrychowicz, Jason Hickey, et al. Deep learning for twelve hour precipitation forecasts. *Nature communications*, 13(1):1–10, 2022.
- Raphael Kriegmair, Yvonne Ruckstuhl, Stephan Rasp, and George Craig. Using neural networks to improve simulations in the gray zone. *Nonlinear Processes in Geophysics*, 29(2):171–181, 2022.
- David A Randall. Beyond deadlock. *Geophysical Research Letters*, 40(22):5970–5976, 2013.
- Yilun Han, Guang J Zhang, Xiaomeng Huang, and Yong Wang. A moist physics parameterization based on deep learning. *Journal of Advances in Modeling Earth Systems*, 12(9):e2020MS002076, 2020.
- Ninghao Liu, Qizhang Feng, and Xia Hu. Interpretability in graph neural networks. *Graph Neural Networks: Foundations, Frontiers, and Applications*, pages 121–147, 2022.
- TN Palmer and DA Mansfield. Response of two atmospheric general circulation models to sea-surface temperature anomalies in the tropical east and west pacific. *Nature*, 310(5977):483–485, 1984.
- Alban Farchi, Patrick Laloyaux, Massimo Bonavita, and Marc Bocquet. Using machine learning to correct model error in data assimilation and forecast applications. *Quarterly Journal of the Royal Meteorological Society*, 147(739):3067–3084, 2021.
- Petar Veličković, Guillem Cucurull, Arantxa Casanova, Adriana Romero, Pietro Lio, and Yoshua Bengio. Graph attention networks. *The Sixth International Conference on Learning Representations*, 2018.

- Yuan Gao, Shohei Miyata, and Yasunori Akashi. Interpretable deep learning models for hourly solar radiation prediction based on graph neural network and attention. *Applied Energy*, 321:119288, 2022.
- Salva Rühling Cachay, Emma Erickson, Arthur Fender C Buckler, Ernest Pokropek, Willa Potosnak, Salomey Osei, and Björn Lütjens. Graph neural networks for improved el niño forecasting. *arXiv preprint arXiv:2012.01598*, 2020.
- Salva Rühling Cachay, Venkatesh Ramesh, Jason NS Cole, Howard Barker, and David Rolnick. Climart: A benchmark dataset for emulating atmospheric radiative transfer in weather and climate models. In J. Vanschoren and S. Yeung, editors, *Proceedings of the Neural Information Processing Systems Track on Datasets and Benchmarks*, volume 1. Curran, 2021.
- Lei Chen, Fei Du, Yuan Hu, Zhibin Wang, and Fan Wang. Swinrdm: Integrate swinrrnn with diffusion model towards high-resolution and high-quality weather forecasting. In *Proceedings of the AAAI Conference on Artificial Intelligence*, volume 37, pages 322–330, 2023a.
- Ryan Keisler. Forecasting global weather with graph neural networks. *arXiv preprint arXiv:2202.07575*, 2022.
- Remi Lam, Alvaro Sanchez-Gonzalez, Matthew Willson, Peter Wirnsberger, Meire Fortunato, Ferran Alet, Suman Ravuri, Timo Ewalds, Zach Eaton-Rosen, Weihua Hu, et al. Learning skillful medium-range global weather forecasting. *Science*, page eadi2336, 2023.
- Jaideep Pathak, Shashank Subramanian, Peter Harrington, Sanjeev Raja, Ashesh Chattopadhyay, Morteza Mardani, Thorsten Kurth, David Hall, Zongyi Li, Kamyar Azizzadenesheli, et al. Fourcastnet: A global data-driven high-resolution weather model using adaptive fourier neural operators. *arXiv preprint arXiv:2202.11214*, 2022.
- Shuo Wang, Yanran Li, Jiang Zhang, Qingye Meng, Lingwei Meng, and Fei Gao. Pm2. 5-gnn: A domain knowledge enhanced graph neural network for pm2. 5 forecasting. In *Proceedings of the 28th international conference on advances in geographic information systems*, pages 163–166, 2020.
- Alexander Y Sun, Peishi Jiang, Zong-Liang Yang, Yangxinyu Xie, and Xingyuan Chen. A graph neural network (gnn) approach to basin-scale river network learning: the role of physics-based connectivity and data fusion. *Hydrology and Earth System Sciences*, 26(19):5163–5184, 2022.
- Peiyuan Li, Yin Yu, Daning Huang, Zhi-Hua Wang, and Ashish Sharma. Regional heatwave prediction using graph neural network and weather station data. *Geophysical Research Letters*, 50(7):e2023GL103405, 2023.
- Martin G Schultz, Clara Betancourt, Bing Gong, Felix Kleinert, Michael Langguth, Lukas Hubert Leufen, Amirpasha Mozaffari, and Scarlet Stadler. Can deep learning beat numerical weather prediction? *Philosophical Transactions of the Royal Society A*, 379(2194):20200097, 2021.
- H. Hersbach, B. Bell, P. Berrisford, G. Biavati, A. Horányi, J. Muñoz Sabater, J. Nicolas, C. Peubey, R. Radu, I. Rozum, D. Schepers, A. Simmons, C. Soci, D. Dee, and J-N. Thépaut. Era5 hourly data on pressure levels from 1959 to present [dataset], 2018.
- Veronika Eyring, Sandrine Bony, Gerald A Meehl, Catherine A Senior, Bjorn Stevens, Ronald J Stouffer, and Karl E Taylor. Overview of the coupled model intercomparison project phase 6 (cmip6) experimental design and organization. *Geoscientific Model Development*, 9(5):1937–1958, 2016.
- Xin Man, Chenghong Zhang, Changyu Li, and Jie Shao. W-mae: Pre-trained weather model with masked autoencoder for multi-variable weather forecasting. *arXiv preprint arXiv:2304.08754*, 2023.
- Franco Scarselli, Marco Gori, Ah Chung Tsoi, Markus Hagenbuchner, and Gabriele Monfardini. The graph neural network model. *IEEE transactions on neural networks*, 20(1):61–80, 2008.
- Stephan Rasp, Peter D Dueben, Sebastian Scher, Jonathan A Weyn, Soukayna Mouatadid, and Nils Thuerey. Weatherbench: a benchmark data set for data-driven weather forecasting. *Journal of Advances in Modeling Earth Systems*, 12(11):e2020MS002203, 2020.
- Stephan Rasp and Nils Thuerey. Data-driven medium-range weather prediction with a resnet pretrained on climate simulations: A new model for weatherbench. *Journal of Advances in Modeling Earth Systems*, 13(2):e2020MS002405, 2021.
- Jonathan A Weyn, Dale R Durran, and Rich Caruana. Improving data-driven global weather prediction using deep convolutional neural networks on a cubed sphere. *Journal of Advances in Modeling Earth Systems*, 12(9):e2020MS002109, 2020.
- Mariana CA Clare, Omar Jamil, and Cyril J Morcrette. Combining distribution-based neural networks to predict weather forecast probabilities. *Quarterly Journal of the Royal Meteorological Society*, 147(741):4337–4357, 2021.
- Tung Nguyen, Johannes Brandstetter, Ashish Kapoor, Jayesh K Gupta, and Aditya Grover. Climax: A foundation model for weather and climate. *arXiv preprint arXiv:2301.10343*, 2023.

- Casper Kaae Søndery, Lasse Espeholt, Jonathan Heek, Mostafa Dehghani, Avital Oliver, Tim Salimans, Shreya Agrawal, Jason Hickey, and Nal Kalchbrenner. Metnet: A neural weather model for precipitation forecasting. *arXiv preprint arXiv:2003.12140*, 2020.
- Ilan Price, Alvaro Sanchez-Gonzalez, Ferran Alet, Timo Ewalds, Andrew El-Kadi, Jacklynn Stott, Shakir Mohamed, Peter Battaglia, Remi Lam, and Matthew Willson. Gencast: Diffusion-based ensemble forecasting for medium-range weather. *arXiv preprint arXiv:2312.15796*, 2023.
- Kang Chen, Tao Han, Junchao Gong, Lei Bai, Fenghua Ling, Jing-Jia Luo, Xi Chen, Leiming Ma, Tianning Zhang, Rui Su, et al. Fengwu: Pushing the skillful global medium-range weather forecast beyond 10 days lead. *arXiv preprint arXiv:2304.02948*, 2023b.
- Kaifeng Bi, Lingxi Xie, Hengheng Zhang, Xin Chen, Xiaotao Gu, and Qi Tian. Accurate medium-range global weather forecasting with 3d neural networks. *Nature*, 619(7970):533–538, 2023.
- Adam Paszke, Sam Gross, Francisco Massa, Adam Lerer, James Bradbury, Gregory Chanan, Trevor Killeen, Zeming Lin, Natalia Gimelshein, Luca Antiga, et al. Pytorch: An imperative style, high-performance deep learning library. *Advances in neural information processing systems*, 32, 2019.
- Dmitrii Kochkov, Janni Yuval, Ian Langmore, Peter Norgaard, Jamie Smith, Griffin Mooers, James Lottes, Stephan Rasp, Peter Düben, Milan Klöwer, et al. Neural general circulation models. *arXiv preprint arXiv:2311.07222*, 2023.
- Noah D Brenowitz and Christopher S Bretherton. Prognostic validation of a neural network unified physics parameterization. *Geophysical Research Letters*, 45(12):6289–6298, 2018.
- Stephan Rasp, Michael S Pritchard, and Pierre Gentine. Deep learning to represent subgrid processes in climate models. *Proceedings of the National Academy of Sciences*, 115(39):9684–9689, 2018.
- Janni Yuval and Paul A O’Gorman. Neural-network parameterization of subgrid momentum transport in the atmosphere. *Journal of Advances in Modeling Earth Systems*, 15(4):e2023MS003606, 2023.
- Oliver Watt-Meyer, Noah D Brenowitz, Spencer K Clark, Brian Henn, Anna Kwa, Jeremy McGibbon, W Andre Perkins, Lucas Harris, and Christopher S Bretherton. Neural network parameterization of subgrid-scale physics from a realistic geography global storm-resolving simulation. *Journal of Advances in Modeling Earth Systems*, 16(2):e2023MS003668, 2024.
- Peidong Wang, Janni Yuval, and Paul A O’Gorman. Non-local parameterization of atmospheric subgrid processes with neural networks. *Journal of Advances in Modeling Earth Systems*, 14(10):e2022MS002984, 2022.
- Dmitry Ulyanov, Andrea Vedaldi, and Victor Lempitsky. Improved texture networks: Maximizing quality and diversity in feed-forward stylization and texture synthesis. In *Proceedings of the IEEE conference on computer vision and pattern recognition*, pages 6924–6932, 2017.
- Deli Chen, Yankai Lin, Wei Li, Peng Li, Jie Zhou, and Xu Sun. Measuring and relieving the over-smoothing problem for graph neural networks from the topological view. In *Proceedings of the AAAI conference on artificial intelligence*, volume 34, pages 3438–3445, 2020.
- Akio Arakawa and Vivian R Lamb. Computational design of the basic dynamical processes of the ucla general circulation model. *General circulation models of the atmosphere*, 17(Supplement C):173–265, 1977.
- ECMWF. Integrated forecasting system. URL <https://www.ecmwf.int/en/forecasts/documentation-and-support/changes-ecmwf-model>.

A Data

We downloaded the preprocessed ERA5 data from <https://dataserv.ub.tum.de/index.php/s/m1524895> Rasp et al. (2020). The 5.625° resolution data is regridded from 0.25° resolution. We use 5.625° resolution dataset for all the experiments in this work.

B Grid to Node Conversion

The process of converting from grids to nodes is shown in Figure 9. The number in each grid represents the node index in the graph. We pad the original area with 32 × 64 grids to 34 × 66 grids, and connect each grid in the original area to its four neighbours (top, bottom, left and right grids). Therefore, the number of nodes in the graph is 32 × 64 + 2 = 2050 in total.

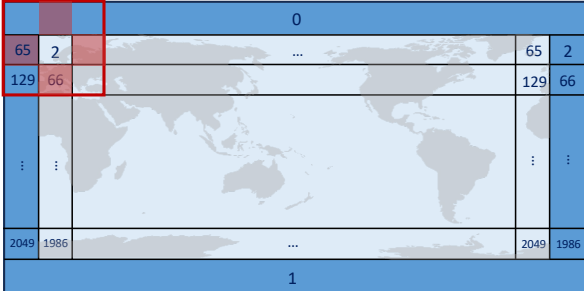


Figure 9: The grid to node conversion. Areas in light blue is the original 32 × 64 grid, and areas in dark blue is the padded grid.

C Codes for Competing Methods

In this study, we use the WeatherBench Rasp et al. (2020), a graph-based model Keisler (2022), and ClimaX Nguyen et al. (2023). The codes are adapted from the source code in GitHub repositories listed in Table 4. The variables used, the training and validation process are identical to our proposed model, after adjusting the parameters and initial learning rate for each model.

Table 4: Source code links for competing methods

Methods	Links
Rasp et al. (2020)	https://github.com/raspstephan/WeatherBench.git
Keisler (2022)	https://github.com/openclimatefix/graph_weather.git
Nguyen et al. (2023)	https://github.com/microsoft/ClimaX.git

C.1 Hyperparameters

Table 5 to Table 7 listed the hyperparameters we use in the competing methods. We mainly adopt the default parameters from the source code, and modify the start learning rate to a suitable value.

D Codes for Calculating Parameters

We use the following codes to calculate the number of parameters for each model.

```
def count_parameters(self):
    return sum(para.numel() for para in self.model.parameters() if para.requires_grad)
```

Table 5: Hyperparameters of WeatherBench Rasp et al. (2020)

Hyperparameter	Value
Image size	[32,64]
Padding	PeriodicPadding
Kernel size	3
Stride	1
Hidden dimension	128
Residual blocks	19
Dropout	0.1
Activation	LeakyReLU

Table 6: Hyperparameters of GraphWeather Keisler (2022)

Hyperparameter	Value
Resolution for h3 mapping	2
Node dimension	256
Edge dimension	256
Number of blocks in message passing	9
Hidden dim in processor node	256
Hidden dim in process edge	256
Hidden layers in processor node	2
Hidden layers in processor edge	2
Hidden dim in encoder	128
Hidden layers in decoder	2

Table 7: Hyperparameters of ClimaX Nguyen et al. (2023)

Hyperparameter	Value
Image size	[32,64]
Patch size	2
Embedding dimension	1024
Number of ViT blocks	8
Number of attention heads	16
MLP ratio	4
Prediction depth	2
Hidden dimension in prediction head	1024
Drop path	0.1
Drop rate	0.1

E Software and Hardware

The model is built with PyTorch Paszke et al. (2019) with the version of PyTorch1.13.1+cu117. The Graph Attention Network is built with PyTorch Geometric 2.4.0. All the experiments are conducted on NVIDIA RTX 4090 GPUs with 24GB memory.